

A novel framework based on deep neural network for determining the melting point of crystalline chemical substances

Anurag Shrivastava ^{*}, Bhavana Shrivastava ⁺

^{*} *Department of Computer Science, Bennett University, Knowledge Park, Greater Noida, India*

⁺ *Department of Computer Science, DIT University, Mussorie Road, Dehradun, India*

Received 6th of December, 2021; accepted 7th of August 2024

Abstract

The melting point detection apparatus is a tool employed in the pharmaceutical and chemical industries to ascertain the melting point of chemical substances. It plays a crucial role in assessing the quality and classification of these substances by identifying their purity or impurities. The proposed framework, which is built upon a deep learning model, utilizes a deep neural network (DNN) incorporating tensorflow, keras, and activation functions. This framework's primary purpose is to classify images representing the state of crystalline chemicals and determine their respective melting points. The class and sub-class labels of crystalline chemical's states were taken into consideration by this deep learning model as a knowledge, which can limit the distance between features in distinct crystalline chemical states images. Additionally, a robust activation function that can fully reserve the image edge features of the chemical's melting region was employed to fit tolerance complete slide image recognition. In the proposed framework activation functions were applied with DNN for the most accurate image classification training purpose. The experiment findings demonstrate that the suggested technique has strong resilience and generalisation, which results in a greater classification accuracy (up to 99.7%) and offers the proposed framework as an effective tool for melting point determination.

Key Words: Deep Neural Network, TensorFlow, Deep Learning, Convolution Neural Network, Keras, Raspberry pi.

1 Introduction

A melting point apparatus is a laboratory instrument employed for the precise and accurate determination of an element's melting point. The melting point is defined as the temperature at which a substance transitions from a solid to a liquid state. Pure substances exhibit a distinct and elevated melting point, whereas impure or contaminated substances typically display a lower melting point and require a longer duration to completely melt, there are various kind of melting point apparatus is being sold in the scientific instruments market, these can be divided in to two categories one is manual process while other is automatic (described in the section 2).

Correspondence to: <nrg.shrivastava@gmail.com>

Recommended for acceptance by <Angel D. Sappa>

<https://doi.org/10.5565/rev/elcvia.1527>

ELCVIA ISSN: 1577-5097

Published by Computer Vision Center / Universitat Autònoma de Barcelona, Barcelona, Spain

1.1 The significance of melting point

The application of melting point apparatus in the pharmaceutical industry is integral for quality control and assurance. This versatile instrument is employed to determine the melting point of pharmaceutical compounds, ensuring their purity and identifying any potential impurities. Accurate melting point analysis plays a pivotal role in confirming the identity of substances, assessing their quality, and validating their integrity in drug formulations. Moreover, it aids in the selection of compatible ingredients during formulation development, monitors the stability of pharmaceutical products, and informs decisions on dosage and release profiles, especially for controlled-release drugs. Additionally, researchers rely on melting point data to investigate the properties of new drug candidates and meet regulatory requirements, ensuring that pharmaceutical products meet stringent quality standards. In essence, the melting point apparatus is a cornerstone of pharmaceutical analysis, contributing to the safety, efficacy, and quality of medications [3].

1.2 Measurement strategy

A systematic strategy for measuring the melting point begins with meticulous sample preparation, ensuring cleanliness and purity. The choice of an appropriate melting point apparatus, calibrated, if necessary, is crucial. Method selection, such as open-tube or closed-tube, should be considered based on the sample and objectives. During experimentation, gradual heating and keen observation are paramount, recording both initial and final melting points and noting any sample behaviour. Repetition of measurements ensures reliability. Post-experiment, data analysis involves calculating the average melting point and comparing it with literature values. A comprehensive report documenting sample details, experimental conditions, and observations guarantees transparency. Implementing stringent validation and quality control measures safeguards the integrity of melting point determination, underpinning its significance in various industries, from pharmaceuticals to chemistry and materials science [12].

1.3 Role of Machine Learning and Artificial Intelligence

There are various kind of automatic melting point apparatus is being sold in the scientific instruments market, these can be divided in to two categories one is manual process while other is automatic, in a manual process based melting point apparatus user has to keep eyes focus on the capillary filled tube till the crystalline chemical substances completely converted into liquid meanwhile user has to watch thermometer for noted down at which temperature chemical substances totally converted in to liquid, the disadvantage of this manual process, user has to switch his attention from capillary to thermometer during switching of user's atension wrong temperature might be noted, and user will not be able to do other task at the same time.

Automatic appratus doesn't require user's attention, user only insert chemical filled capillary tube into apparatus and switch on the device when a device gets the melting point, device start alarming. These appratus are based on the reflectancenss and transmittance of light and others are based on image processing-based methods. In reflectanceness and transmittance of light-based apparatus determined the melting point throughout changing in the light transmission by optical light sensor while Computer vision based apparatus used change detection algorithms for determining the melting point.

Deep learning is among the most powerful techniques in artificial intelligence. It's a form of AI that can mimic human-like behavior and thinking. To make the "training" session more effective and quicker, the system is typically configured with hundreds or even thousands of input data. It begins by 'training' the system with all the inputs [1].

Deep learning is now widely used in various domains, including pattern recognition, change detection, natural language processing, social network filtering, speech recognition, machine translation, and bioinformatics.

It often produces results that are on par with, and in few cases, superior to those of human experts. It learns with neural networks that have more than one hidden layer to improve image classification performance. It has evolved into indispensable for image classification [11].

Methods and algorithms for change detection operate by analyzing the intensity values of pixels at specific locations within a capillary filled tube. During the process of filling the capillary tube with chemicals, air bubbles may inadvertently form at these locations then these methods may produce inaccurate results[8] while CNNs architecture has a high learning capacity and identify the nature of an input image without any prior information, thus they're a good choice for image classification, the proposed framework, employed a deep neural network, build an application and distribute it on a Raspberry Pi board. It aims to identify the melting points of chemical compounds.

1.4 Profitable approach

A deep learning-based approach for melting point determination holds the potential for profitability due to its transformative impact on traditional methods. By leveraging advanced algorithms, it can automate the measurement process, significantly increasing efficiency and reducing the need for skilled labor. This not only saves time but also lowers labor costs, contributing to overall cost-effectiveness. Furthermore, the accuracy and precision offered by deep learning models enhance the reliability of research results and product quality control, reducing the risk of errors and costly rework. Customization capabilities allow the apparatus to handle a wide range of sample types, appealing to diverse customer needs. As a cutting-edge technology, it can command premium pricing, attracting customers who value precision and automation. Intellectual property opportunities through proprietary algorithms and the potential for maintenance and support services further bolster profitability. In a competitive market driven by the demand for accurate temperature measurement in research and industry, a deep learning-based approach can position itself as a valuable and profitable solution.

1.5 Significance and advantages of this research

A deep learning-based melting point apparatus can be a valuable tool in the field of chemistry and pharmaceutical industry, offering several potential benefits and profit opportunities:

- **Automation and Efficiency:** Deep learning algorithms can automate the process of melting point determination, reducing the need for manual intervention. Faster and more efficient measurements can lead to increased productivity in research and quality control labs.
- **Accuracy and Precision:** Deep learning models can enhance the accuracy and precision of melting point measurements by analyzing data more objectively and consistently than human operators. This can improve the reliability of research results and product quality control.
- **Reduced Labor Costs:** Automation through deep learning can reduce the need for skilled personnel to perform melting point determinations, leading to potential labor cost savings.
- **Data Analysis and Insights:** Deep learning algorithms can analyze large datasets generated during melting point experiments and provide insights that may not be readily apparent through traditional methods. Researchers can gain a deeper understanding of the properties of materials.
- **Competitive Advantage:** Offering a deep learning-based melting point apparatus can differentiate your product from competitors, attracting customers looking for advanced, automated solutions. Such innovation can enhance brand's reputation in the scientific community.
- **Intellectual Property:** Developing proprietary deep learning algorithms for melting point analysis could lead to patents and licensing opportunities, creating an additional revenue stream.

- Collaborations and Partnerships: Collaborating with research institutions and universities to refine and validate deep learning models can enhance credibility and generate research grants or partnerships.
- Market Expansion: By offering a sophisticated and accurate melting point apparatus, may tap into new markets and industries where precise temperature measurement is critical.

Profitability in this venture would depend on various factors, including the initial investment in research and development, manufacturing costs, pricing strategy, and the demand for such technology in the market. Conducting market research and understanding the specific needs of potential customers can help gauge the profitability of a deep learning-based melting point apparatus in target market. Additionally, ensuring regulatory compliance and adhering to quality standards is essential for long-term success in this field.

1.6 Traditional method & significant findings in the work

In the conventional methods for determination of the melting point, the standard procedure involves taking two to five grams of chemical substance in powdered form and transferring an appropriate amount of the powdered chemical into a capillary tube. The tube is then tapped gently on a stable surface to settle the powder. Subsequently, the procedure of heating is initiated using a small fire stove, with the temperature gradually increased. The melting point of the chemical substance is defined as the temperature at which the crystalline chemical in powdered form completely transforms into a liquid state. This method is based on the principles outlined in reference [12].

In traditional melting point apparatus user has to keep eyes focus on capillary filled tube till the crystalline chemical substances completely converted into liquid meanwhile user has to watch thermometer for noted down at which temperature chemical substances totally converted in to liquid, the disadvantage of this manual process, user has to switch his attention from capillary to thermometer during switching of user's attention wrong temperature might be noted, and user will not be able to do other task at the same time.

In next generation of melting point apparatus also known as automatic apparatus doesn't require user's attention, user only insert chemical filled capillary tube into apparatus and switch on the device when device gets the melting point, device start alarming. These apparatuses are based on image processing-based methods and uses change detection algorithms.

Methods and algorithms for change detection operate by analyzing the intensity values of pixels at specific locations within a capillary filled tube. During the process of filling the capillary tube with chemicals, air bubbles may inadvertently form at these locations then these methods may produce inaccurate results while CNNs architecture has a high learning capacity and identify the nature of an input image without any prior information, thus they're a good choice for image classification, the proposed framework, employed a deep neural network, build an application and distribute it on a Raspberry Pi board. It aims to identify the melting points of chemical compounds once the proposed model is trained using the DCSS image dataset. Additionally, it classifies real-time images taken from the camera into two categories: solid state and liquid state. When the proposed model receives an image of a chemical in liquid form, the current temperature in degree Celsius referred to as the melting point. Afterward, an evaluation of the proposed model's performance conducted, and the discussion of its performance presented in the results section.

Deep learning and Convolutional Neural Networks (CNNs) are closely related, as CNNs are a specific type of neural network architecture used within the field of deep learning for tasks related to image processing and pattern recognition. Deep learning is a subset of machine learning, dedicated to the training of neural networks comprising multiple layers, known as deep neural networks. These networks are designed to autonomously acquire hierarchical data representations. These networks can learn to extract features from raw data, make

predictions, and perform various tasks, including image classification, object detection, natural language processing, and more.

Convolutional Neural Networks (CNNs) are a class of deep neural network architectures crafted for the analysis of grid-like data, primarily images. Drawing inspiration from the human visual system, CNNs encompass various layers, including convolutional layers, pooling layers, and fully connected layers. CNNs are particularly proficient in capturing spatial hierarchies of features within images.

In this paper, a novel framework, utilizing a Convolutional Neural Network (CNN), has been proposed and developed in Python. It leverages supporting libraries and tools, including TensorFlow and Keras, for determination of the melting point of crystalline chemical substances. Additionally, this framework can be deployed on various platforms, including computers, tablets, or single-board computers like Asus Tinker Board or Raspberry Pi. In the proposed work, Raspberry Pi has been employed.

This article is structured as follows: Section 1 introduces the topic, Section 2 presents related research, Section 3 describes the proposed framework methodology, Section 4 is dedicated to experimental analysis, and Section 5 presents the results of the proposed model. The conclusion is provided in Section 6.

2 Literature review

The melting point of a completely pure solid organic compound is a unique intrinsic attribute, akin to characteristics such as molecular weight, boiling point, refractive index, and density. A pure solid substance displays a consistently reliable melting behaviour over a relatively narrow temperature range, typically within 1°C or less. This determination of the melting characteristic is performed on an extremely small scale, requiring less than 1 mg of the substance. The equipment used for this purpose is simple, involving just a thermometer, a capillary tube for holding the sample, and a heating bath. Melting points serve three fundamental roles: Firstly, in the case of a known compound, determining its melting point aids in the characterization of the current sample. Secondly, for newly discovered compounds, recording the melting point is essential for enabling future characterizations by other researchers. Lastly, the melting point range offers insights into the purity of the compound; impure substances exhibit a broad melting range. Through recrystallization, the compound can be purified, resulting in a narrower melting point range and a shift towards higher temperatures. For instance, an impure sample might initially melt between 124-126°C but, after recrystallization, exhibit a narrower range of 125-125.5°C. A solid is deemed pure if its melting point remains unaltered following recrystallization [3].

The approaches to determine melting points can be categorized into two main groups: traditional manual methods and contemporary automatic methods. Various types of melting point apparatus have been developed in accordance with these methodologies. This description delves into the current methodologies.

2.1 Traditional methods

In the manual procedure, the established protocol for melting point determination begins with the transfer of two to five grams of chemical substances in powdered form into a capillary tube. After carefully filling the tube with the powdered chemical. Subsequently, the heating process commences using a small fire stove, with the temperature increasing gradually. The melting point of the chemical substance is defined as the temperature at which the powdered crystalline material completely transforms into a liquid state [3]. Throughout this procedure, the user must maintain their attention on the capillary tube to observe the substance's state and on the thermometer to track the temperature. However, this process requires the user to switch their attention between the capillary and the thermometer, potentially affecting the accuracy of the results. In this method, the accuracy depends entirely on human attention and judgment. These types of apparatus lack digital features such as timers, digital temperature displays, and options for recording the entire melting process. The apparatus

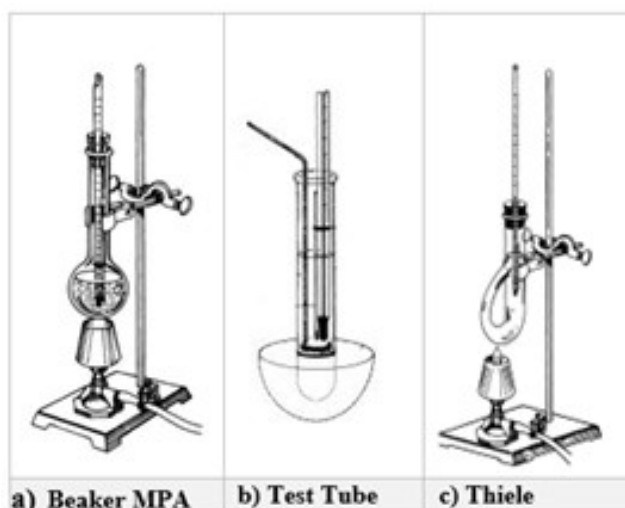


Figure 1: Types of Traditional Melting Point Apparatus (MPA)

shown in Figure 1, including the Beaker MPA, Test Tube, and Thiele tube, are examples based on this method. In contrast, the proposed approach, based deep learning techniques, can automatically determine the melting point without the need for human intervention. Users can engage in other tasks simultaneously, and the result's accuracy is not reliant on human attention and judgment.

2.2 Modern methods

Apparatus employing electrical heating employ a range of sensors to ascertain the melting point. To accomplish this, the capillary tube and thermometer are inserted into a metal block. A transformer is employed to regulate the temperature and control the heating rate of the metal block. Subsequently, the reading is examined using a connected magnifying lens [12]. Examples of such apparatus include the Thomas Hoover Uni Melt and the Mel-Temp devices.

The Thomas-Hoover Uni-Melt and Mel-Temp instruments feature a compact, magnified, and illuminated chamber that can accommodate seven capillaries, shown in figure 2. This chamber is filled with high-boiling-point silicone oil, which is electrically heated and circulated. The devices are equipped with a variable transformer to regulate the heating rate. When paired with a specialized thermometer, these instruments can operate at temperatures as high as 500°C, exceeding the heating range of apparatuses using silicone oil, which is typically limited to 350°C. Furthermore, the device is equipped with a digital thermometer [12].

In these types of apparatus, the primary detection method relies on human observation, necessitating users to follow the same operational procedure and demanding their full attention. Consequently, the issue remains unresolved.

The computer-aided optical sensor approach, which emulates human vision, revolves around assessing light transmittance through a sample. It eliminates the necessity for closely calibrated devices. This technique entails the placement of a capillary tube with roughly 3 mg. of chemical in the optical way of a system. This system guides light passes throughout the filled capillary tube and projects it onto a group of photoresistors. The patterns captured on these group depends on the structural characteristics of the chemical and register alterations as the crystals modify their shapes. Subsequently, the system selects frames from the group and calculates the rate of pattern transformation [6]. In this apparatus, human attention is not required as it determines the melting point automatically. However, there may be occasional discrepancies in the results due to the presence of

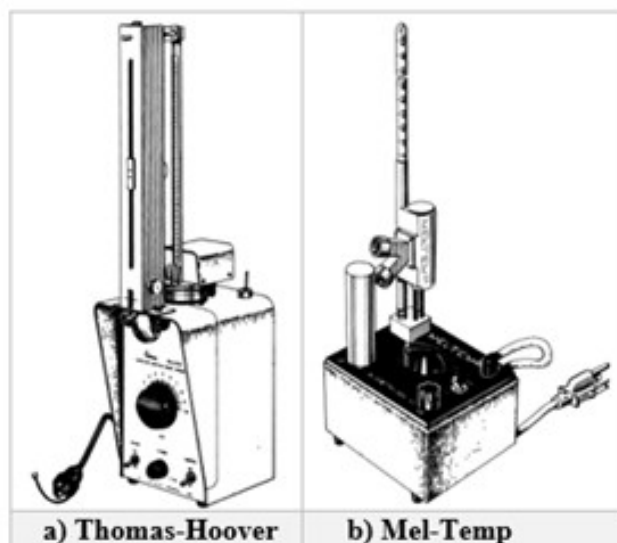


Figure 2: Electric sensors-based Apparatus (MPA)

bubbles of air within the capillary tube. Its design is highly intricate, and the sensors are costly. The maximum achievable accuracy is 98.70% [6].

The Melting-Point-Detector (MPD) algorithm was utilized to analyse changes in pixel values. This algorithm consistently calculates the value representing the intensity of a pixel at a particular location within a capillary image and detects the differences in intensity values between two consecutive images. When a phase transition in a chemical substance takes place at a specific instance, and the discrepancy in pixel's intensity value exceeds a predefined threshold, the current running temperature is logged as the melting point of crystalline chemical compounds [8]. The MPD algorithm produces precise outcomes. Nevertheless, the only limitation of this approach arises when an air bubble becomes trapped among the chemical crystals at a position where the MPD algorithm calculates pixel values, potentially leading to result discrepancies. The maximum accuracy achieved by the MPD algorithm is 98.8% [8].

2.3 Deep learning and Machine learning methods

A new methodology has been introduced to predict the melting process of CZ monocrystalline silicon using Convolutional Neural Network (CNN) deep learning techniques. This approach combines deep learning methodologies with the classification of melting process images. Focusing on CNN, a melting classification model based on AlexNet has been developed, ultimately leading to the establishment of a CNN-based model for classifying melting stages. Experimental results affirm the model's ability to effectively predict silicon's melting process with a remarkable 98.5% accuracy, underscoring its practical viability [13].

A deep learning model has been developed for predicting the melting point (T_m) of diverse ionic liquids (ILs) composed of various cation and anion combinations. This model enables accurate T_m predictions, achieving a high level of accuracy with an R^2 score of 0.90 and a root mean square error (RMSE) of approximately 32 K. The melting points of ILs are primarily influenced by key molecular descriptors, which can serve as valuable guidelines for refining the T_m of ILs [2].

In this study, the authors investigated a data-driven approach employing machine learning (ML) techniques to predict and gain insights into the melting points of molecules. They compiled data from various experimental

databases found in the literature to create a minimally biased dataset, encompassing 3D structural and quantum-chemical properties. By taking into account experimental variability and polymorph-induced uncertainties, they established a reliable lower threshold for predicting melting points and employed graph neural networks and Gaussian processes to make predictions that are competitive with these predefined accuracy bounds. Additionally, to gain a deeper understanding of how melting points relate to molecular structure, they utilized several semi-supervised and unsupervised ML methods [10].

The authors employed the k-nearest neighbor (kNN) modelling technique to make predictions regarding melting points. They utilized two datasets: one consisting of 4119 diverse organic molecules (dataset 1) and another containing 277 drugs (dataset 2). These datasets were employed to assess performance across different areas of chemical space. The authors also explored the impact of adjusting the number of nearest neighbor while employing various types of molecular descriptors. In order to predict melting temperatures based on the temperatures of the nearest neighbor, four distinct methods were applied, including arithmetic and geometric averaging, inverse distance weighting, and exponential weighting. Notably, the exponential weighting method delivered the most promising results. The optimized model achieved an average root mean square error (RMSE) as low as 46.2 degrees Celsius, accompanied by an r^2 value of 0.49 [7].

2.4 The research gaps

J. Zhang, et. Al [13]. Authors have designed a Convolutional Neural Networks (CNN) to predict the melting point of CZ monocrystalline silicon. An AlexNet-based classification model was developed, achieving 98.5% accuracy in predicting of melting point, also demonstrated practical effectiveness. CZ (Czochralski) monocrystalline silicon finds widespread use in the electronics and semiconductor industries, serving as a foundational material for a range of critical applications. Its high purity and uniform crystal structure make it ideal for semiconductor manufacturing, where it is the primary material for integrated circuits and solar cells. CZ silicon also plays a key role in solar photovoltaics, enabling the production of high-efficiency solar panels.

Mainly, their work was related to the electronics industry. The authors used a CNN-based model to predict the melting point of CZ monocrystalline silicon. There is potential for utilizing a CNN-based model for determining the melting point of chemical compound which are in powdered form, which could lead to revolutionary research and innovation in the pharmaceutical industry. Moreover, there is room for improving the model's accuracy. It would be more valuable to determine the melting point in real-time rather than predicting it.

Change detection based MPD algorithms work on pixels' intensity value at particular location of capillary filled tube, during chemical filling in capillary tube air bubble might come at those location then these methods may produce inaccurate results [9] while CNNs architecture has a high learning capacity and identify the nature of an input image without any prior information, thus they're a good choice for image classification, Using this approach, an ergonomic melting point apparatus may be designed.

3 Proposed methodology

The proposed methodology mainly consists of three main parts: a) The proposed model b) Implementation of the proposed model, including the development of an application and c) Assembly of an experimental setup within a dark box.

The proposed framework has a significant capacity for learning along with the inter class distance constraints of images of chemical's state. The proposed framework, which has several hidden layers gets the learning from inherent features and constraints. The convolution utilized as a feature extraction technique and input signal in

the proposed framework is the critical computation. Each neuron computes a dot product between its weights and the input volume region to which it is connected in the convolutional layer. This computation determines the output of neurons associated with specific regions in the input.

3.1 The proposed model based on CNN

The proposed model was developed for classifying the melting stage. The network architecture was fine-tuned through experimental iterations, involving adjustments to the counting of convolution layers and kernel sizes. The final melting stage classification model comprised four CNN layers and two layers are fully-connected. Each CNN layer had two components: a convolutional layer and, optionally, a pooling layer.

The convolution layer possesses strong feature extraction capabilities, and the pooling layer serves to decrease the dimensionality of the feature map, simplifying the network's computational complexity. The fully connected layer consolidates the extracted feature information, transforming two-dimensional data into a one-dimensional format, which is conducive to achieving the ultimate classification task.

The convolution layer employed the ReLU activation function, and the final output layer utilized a softmax activation function. Detailed descriptions of each layer within the network follow.

- The input layer: After processing the original image, a pixel matrix of dimensions $227 \times 227 \times 3$ was acquired.
- The 1st convolutional layer: Within this segment, the first layer is a convolutional layer. It employs a set of 64 convolution kernels, each measuring 11×11 , and advances with a stride of 4. As the input frame consists of pixel values in RGB format across three channels, the number of convolution kernels are 64 within this layer are likewise 3 channels. Consequently, the features map size following the CNN in this layer is calculated as one plus the result of dividing the difference between 227 and 11 by 4, resulting in a total of 64 feature maps, each measuring a square with sides of length 55 units each.
- The 2nd layer is the pooling layer, which processed the sixty-four feature maps, each with dimensions 55×55 , generated by the CNN. The pooling is conducted using a 3×3 window, with a stride of 2. This yielded a pooled features map size calculated as $1 + ((55 - 3) / 2)$, resulting in a total of 64 feature maps, each with a size of 27 by 27.
- The 2nd convolutional layer: Second convolutional layer was equipped with 64 kernels, each measuring 3×3 , and it employed a stride of 1. Additionally, zero-padding was applied. As a result, the size of the dimension of the feature map following CNN in this layer calculated as $(27 - 3 + 2 \times 1) / 1 + 1$, ultimately yielding sixty-four feature maps, each with dimensions of 27 by 27.
- the 2nd layer of pooling, which conducted pooling on the sixty-four feature maps, each sized 27×27 , derived from the CNN. Employing a 3×3 pooling window with a stride of 2, the size of the pooled feature map was computed as $(27 - 3) / 2 + 1$, resulting in sixty-four feature maps, each measuring 13 by 13.
- The 3rd convolutional layer: In this layer, 64 convolution kernels sized 3×3 were employed with a stride of 1. Zero-padding was applied, resulting in the feature map size after convolution being calculated as $(13 - 3 + 2 \times 1) / 1 + 1$, yielding sixty-four feature maps, each measuring 13 by 13. Notably, this layer did not include any pooling operations.
- The 4th convolutional layer: The fourth convolutional layer featured 64 kernels, each with dimensions of 3×3 , and used a stride of 1. Zero-padding was applied, resulting in a feature map size calculated as $(2 + 13 - 3) / 1 + 1$, producing sixty-four feature maps, each measuring 13×13 . Following this was a pooling layer, which operated on the sixty-four feature maps, sized 13 by 13, obtained from the CNN. Employing

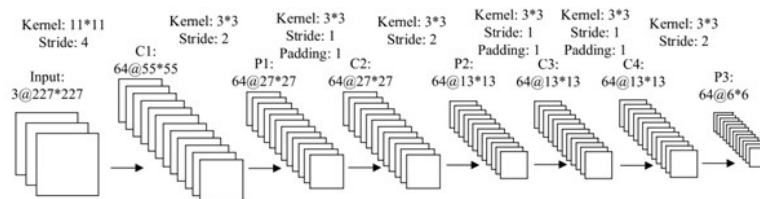


Figure 3: A Convolutional Neural Network for classification of chemical substances' states. In the diagram, C denotes the convolutional layer, and P designates the pooling layer. The numeric value preceding @ denotes the quantity of feature maps, while the number following the symbol denotes the dimensions of each individual feature map. 'Kernel' specifies the size of the convolutional kernel, 'Stride' indicates the step of movement, and 'Padding' defines the extent of zero-padding applied.

a 3×3 pooling window with a stride of 2, the pooled feature map size was calculated as $(13 - 3) / 2 + 1$, resulting in 64 feature maps, each with dimensions of 6 by 6.

- The 1st fully connected layer: It consisted a total of 512 neural units. Initially, the sixty-four feature maps, each measuring 6 by 6 and derived from the preceding four convolutional layers, transformed into a vector with a single dimension, comprising a total of 2,302 neural units. This one-dimensional vector was fully connected to the 512 neurons, following a similar approach to a backpropagation.
- The 2nd fully connected layer: Given the binary classification nature of the task, the second fully connected layer was equipped with 2 neurons. The output from the 512 neurons in the 1st fully connected layer was fully connected to the 2 neurons in this layer. To generate probability outputs indicating membership in each category, the softmax function was employed by each neuron.
- The CNN classification model's architecture is presented in figure 3, with the pooling layer not explicitly depicted. The comprehensive process for establishing the classification model was elucidated during the experimentation phase.

3.2 Dataset

The proposed work has employed its own image-dataset, referred to as the Dataset of Chemical Substances' States (DCSS). Consisting of image of capillaries filled with chemical obtained through real-time video capturing during the manual process of determining the melting points of these substances. These images were categorized into two class labels, the first being the type of image belonged to the liquid class label and the second category to the solid class, the samples of these images are shown in Figure 4.

The DCSS dataset contains a total of 2500 images depicting phase transitions of crystalline chemical substances. Out of these, 1178 images represent the liquid phase, while 1322 images represent the solid state. These images are fed into the proposed model for training purposes. Once the model is trained, it categorizes these images into two class labels and determines the melting points of chemical substances.

4 Experimental analysis

The experimental setup consisted of several essential components, which included a capillary tube, an aluminium heater block, a cartridge heater, a proposed DNN-based model, a temperature sensor, a single-board computer (Raspberry Pi), and the chemical substance D-glucose. These elements were meticulously arranged within a light-tight enclosure, creating a unified system with the purpose of determining the melting point of

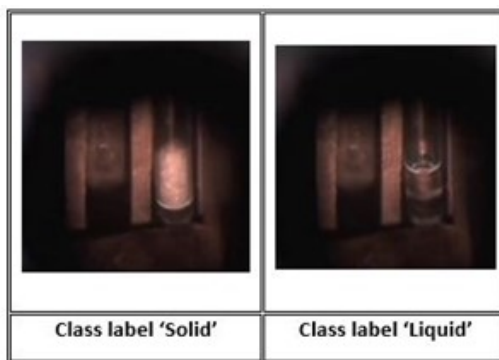


Figure 4: The sample image of DCSS dataset

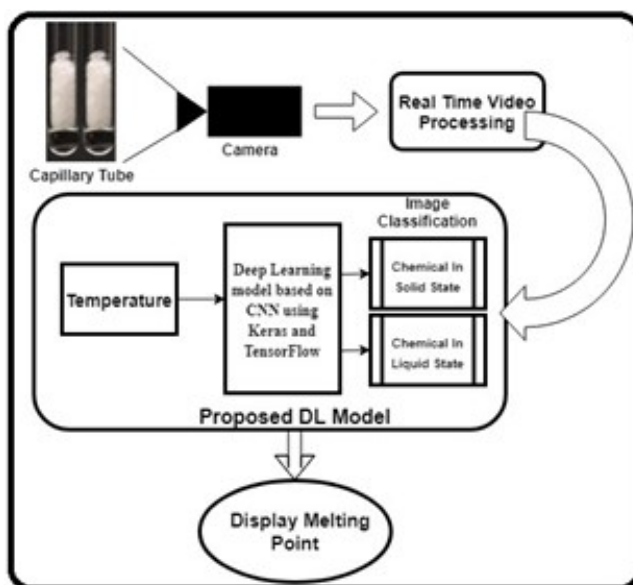


Figure 5: Proposed experimental setup for measuring the melting point of chemical compounds

powdered D-glucose. The procedure commenced by filling the capillary tube with D-glucose, which was then delicately positioned on top of the aluminium heater block. Subsequently, the block was heated using a cartridge heater connected to a DC power supply, the graphical representation of the entire experimental setup is shown in Figure 5, and the box containing the assembly for melting point determination is shown in Figure 6.

The proposed framework, implemented in Python, has been developed as an application and installed on a single-board computer (Raspberry Pi). This system initiated the process by capturing real-time images of capillary tubes filled with chemical substances using an integrated camera. These images were then transmitted to the proposed framework, which performed classification into two categories, distinguishing whether the chemical substances were in a liquid or solid state. Simultaneously, the capillary containing the chemical substances was positioned above a heated block and subjected to continuous heating through an electric cartridge heater operated by an electric circuit. Whenever the proposed framework identified an image containing the chemical in a liquid state, the current temperature was recorded in memory and considered as the melting point of the chemical substance.

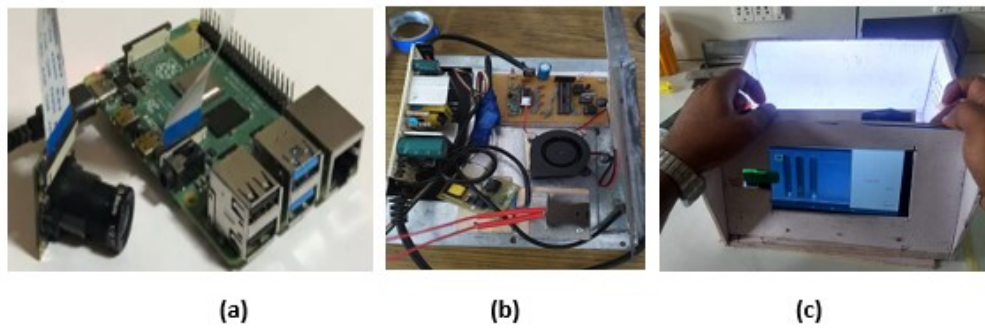


Figure 6: (a) The image of single board computer (Raspberry PI) with camera module, (b) The image of a wooden box enclosed electric circuitry with heater block, (c) The image of screen for displaying the entire melting process.

4.1 Programming logic framework

The suggested model was developed using Python, and the outcomes were subjected to analysis. The implementation encompassed the following steps: Initially, two directories named 'solid' and 'liquid' were established, housing frames of chemical substances in powdered solid and liquid states for the purpose of training. These images were generated from the DCSS dataset, and the 'imagedatagenerator' library was employed for labelling all the images within the 'solid' and 'liquid' directories. To load frames into the proposed model, the `img = image.load_img(path)` method was employed. The '`cv2.imread(path)`' function was also used to ascertain the three-dimensional matrix shape, providing information about image size as (408, 402, 3), where 408 px denotes the height, 402 px signifies the width, and 3 denotes a 3-dimensional matrix.

The training and validation process involved initializing two classes for training and validation within the programming to generate training images using the 'imagegenerator.' Despite the RGB pixel values ranging from 0 to 255, it was necessary to convert these values to a range between 0 and 1 by rescaling. This involved dividing each pixel value by 255, which was achieved through the '`rescale = 1/255`' function. The same procedure was applied to the validation class.

The proposed model utilized the training images by inputting them into the convolution neural network through the `train.flow_from_directory` function. The training class images had varying sizes, enabling the utilization of images of different dimensions within the neural network. Nonetheless, it was imperative to resize these images using the `target_size` method, and the resized frames were standardized to (200, 200) pixels. Furthermore, it was vital to specify the class mode, and in the proposed model, the binary class mode was employed. The same procedure was replicated for the validation class, the entire process flow diagram of the proposed framework is shown in Figure 7.

The convolution neural network didn't use string labels; it represented classes with numerical values. The two image classes were denoted as either '0' or '1', with 'liquid': 0, 'solid': 1. After defining the training and validation datasets, the proposed model employed a convolutional neural network with the max-pool activation function. The layers were added sequentially using `tf.keras.models.Sequential` in the code. The `Sequential` function arranged the layers in a sequential order.

Utilizing `Conv2D` along with `Maxpool2D`, which selects the maximum pixel values, and incorporating a `flatten` layer for converting multidimensional data into a single-dimensional array. Ultimately, a `Dense` layer was applied to consolidate the outputs from the previous layers into neurons, where each neuron passes its output to subsequent layers.

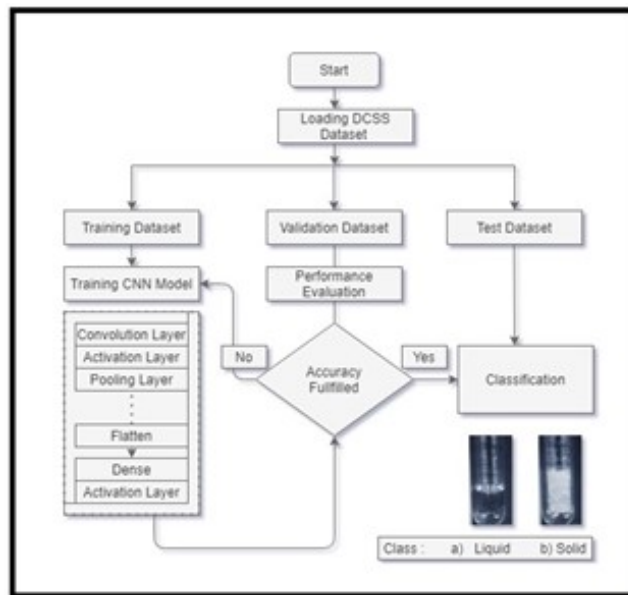


Figure 7: A process flow diagram for the proposed framework

5 Results

Deep learning-based models are becoming increasingly popular because they produce outstanding results and provide an effective solution for evaluating large amounts of data. TensorFlow and Keras, with various activation functions, were employed in the proposed framework to classify images taken from the DCSS image dataset. For performance testing of the proposed framework, we calculated model accuracy, validation accuracy, training loss, and model loss with and without the utilization of activation functions such as ReLu and sigmoid on 15, 20, and 25 epochs and compared performance with previously used deep learning-based models for predicting the melting point of CZ monocrystalline silicon [13], classifying fake news [4], and breast cancer image classification [5].

We have meticulously developed the complete Python code for implementing the proposed framework within the Jupyter IDE. Key metrics, including model loss, model accuracy, validation loss, and validation accuracy at each step of the aforementioned epochs used for assessing the performance of the proposed model, are expressed as percentages by Jupyter IDE and are presented in the output frame.

Six trials in total were considered: three of them utilized activation functions for 15, 20, and 25 epochs, respectively, while the remaining three did not employ activation functions on the DCSS image dataset. The results of these trials are shown in Figures 8, 10, and 12, respectively. Additionally, graphical representations of model loss and model accuracy can be found in Figures 9, 11, 13, 14, 15, and 16, respectively. Ultimately, this analysis demonstrated that increasing the epoch count with an activation function led to achieving a maximum training accuracy of 99.7% and a maximum model validation accuracy of 99.3%.

Table 1 displays the maximum training accuracy, maximum validation accuracy, maximum training loss, and maximum validation loss of the proposed framework with and without the utilization of an activation function. This analysis suggests that increasing the number of epochs with the activation function leads to a maximum accuracy of 99.7%, while the maximum validation accuracy on the DCSS image dataset reached 99.3%.

J. Zhang, et. al [13], authors have used Convolutional Neural Networks (CNN) to predict the melting point of CZ monocrystalline silicon, W. Han et. al [4], they have used prominent deep learning techniques, such hybrid CNN and RNN for fake news detection, and N. Syahmi et. al. [5], They assess the capacity of the

```

Epoch 3/15 ..... 30 10/17500 - loss: 0.8264 - accuracy: 0.7778 - val_loss: 0.7942 - val_accuracy: 0.8048
Epoch 4/15 ..... 30 10/17500 - loss: 0.7904 - accuracy: 0.8004 - val_loss: 0.8270 - val_accuracy: 0.8048
Epoch 5/15 ..... 30 10/17500 - loss: 0.8386 - accuracy: 0.7778 - val_loss: 0.8261 - val_accuracy: 0.8048
Epoch 6/15 ..... 30 10/17500 - loss: 0.8158 - accuracy: 0.8000 - val_loss: 0.8068 - val_accuracy: 0.8048
Epoch 7/15 ..... 30 10/17500 - loss: 0.8484 - accuracy: 0.8000 - val_loss: 0.8222 - val_accuracy: 0.8048
Epoch 8/15 ..... 30 10/17500 - loss: 0.8484 - accuracy: 0.7778 - val_loss: 0.8484 - val_accuracy: 0.8048
Epoch 9/15 ..... 30 10/17500 - loss: 0.8523 - accuracy: 0.8071 - val_loss: 0.8231 - val_accuracy: 0.8048
Epoch 10/15 ..... 30 10/17500 - loss: 0.8524 - accuracy: 0.7778 - val_loss: 0.8484 - val_accuracy: 0.8048
Epoch 11/15 ..... 30 10/17500 - loss: 0.8428 - accuracy: 0.8487 - val_loss: 0.8428 - val_accuracy: 0.8048
Epoch 12/15 ..... 30 10/17500 - loss: 0.8033 - accuracy: 0.8487 - val_loss: 0.8033 - val_accuracy: 0.8048
Epoch 13/15 ..... 30 10/17500 - loss: 0.8193 - accuracy: 0.8000 - val_loss: 0.8170 - val_accuracy: 0.8048
Epoch 14/15 ..... 30 10/17500 - loss: 0.8294 - accuracy: 0.8000 - val_loss: 0.8492 - val_accuracy: 0.8048
Epoch 15/15 ..... 30 10/17500 - loss: 0.8294 - accuracy: 0.7778 - val_loss: 0.8489 - val_accuracy: 0.8048
Epoch 16/15 ..... 30 10/17500 - loss: 0.8229 - accuracy: 0.8000 - val_loss: 0.8295 - val_accuracy: 0.8259
fit_metrics['loss', 'accuracy', 'val_loss', 'val_accuracy']:
Epoch 3/20 ..... 40 30/17500 - loss: 11.9972 - accuracy: 0.2222 - val_loss: 11.8289 - val_accuracy: 0.2489
Epoch 4/20 ..... 40 30/17500 - loss: 11.9972 - accuracy: 0.2222 - val_loss: 11.8289 - val_accuracy: 0.2489
Epoch 5/20 ..... 40 30/17500 - loss: 10.2023 - accuracy: 0.3333 - val_loss: 11.8289 - val_accuracy: 0.2489
Epoch 6/20 ..... 40 30/17500 - loss: 10.2023 - accuracy: 0.3333 - val_loss: 11.8289 - val_accuracy: 0.2489
Epoch 7/20 ..... 40 30/17500 - loss: 11.7211 - accuracy: 0.3333 - val_loss: 11.8289 - val_accuracy: 0.2489
Epoch 8/20 ..... 40 30/17500 - loss: 11.7211 - accuracy: 0.3333 - val_loss: 11.8289 - val_accuracy: 0.2489
Epoch 9/20 ..... 40 30/17500 - loss: 11.7211 - accuracy: 0.3333 - val_loss: 11.8289 - val_accuracy: 0.2489
Epoch 10/20 ..... 40 30/17500 - loss: 11.7211 - accuracy: 0.3333 - val_loss: 11.8289 - val_accuracy: 0.2489
Epoch 11/20 ..... 40 30/17500 - loss: 10.2023 - accuracy: 0.3333 - val_loss: 11.8289 - val_accuracy: 0.2489
Epoch 12/20 ..... 40 30/17500 - loss: 10.2023 - accuracy: 0.3333 - val_loss: 11.8289 - val_accuracy: 0.2489
Epoch 13/20 ..... 40 30/17500 - loss: 10.2023 - accuracy: 0.3333 - val_loss: 11.8289 - val_accuracy: 0.2489
Epoch 14/20 ..... 40 30/17500 - loss: 10.2023 - accuracy: 0.3333 - val_loss: 11.8289 - val_accuracy: 0.2489
Epoch 15/20 ..... 40 30/17500 - loss: 10.2023 - accuracy: 0.3333 - val_loss: 11.8289 - val_accuracy: 0.2489
Epoch 16/20 ..... 40 30/17500 - loss: 10.2023 - accuracy: 0.3333 - val_loss: 11.8289 - val_accuracy: 0.2489
Epoch 17/20 ..... 40 30/17500 - loss: 10.2023 - accuracy: 0.3333 - val_loss: 11.8289 - val_accuracy: 0.2489
Epoch 18/20 ..... 40 30/17500 - loss: 10.2023 - accuracy: 0.3333 - val_loss: 11.8289 - val_accuracy: 0.2489
Epoch 19/20 ..... 40 30/17500 - loss: 10.2023 - accuracy: 0.3333 - val_loss: 11.8289 - val_accuracy: 0.2489
Epoch 20/20 ..... 40 30/17500 - loss: 10.2023 - accuracy: 0.3333 - val_loss: 11.8289 - val_accuracy: 0.2489
fit_metrics['loss', 'accuracy', 'val_loss', 'val_accuracy']:
    
```

Figure 8: The accuracy of the proposed framework at each iteration during the 15 epochs with activation function shown on left side and without using activation function shown in right side

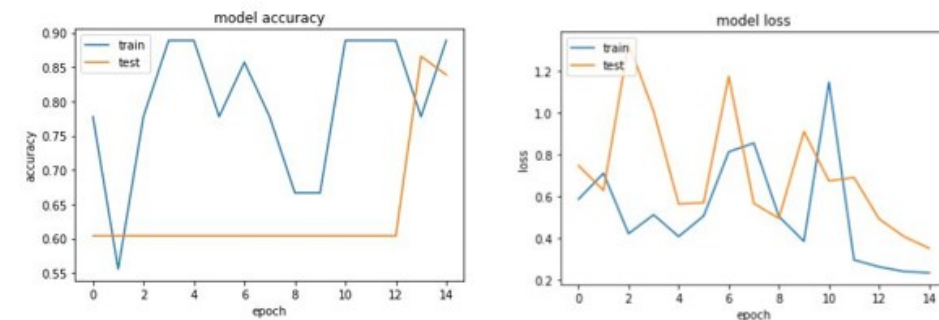


Figure 9: The graph plotting for model accuracy and loss in the proposed framework, involving the use of activation functions, was conducted over 15 epochs.

```

Epoch 3/20 ..... 40 30/17500 - loss: 0.8221 - accuracy: 0.3333 - val_loss: 0.8482 - val_accuracy: 0.7131
Epoch 4/20 ..... 40 30/17500 - loss: 0.8386 - accuracy: 0.3333 - val_loss: 0.8262 - val_accuracy: 0.7131
Epoch 5/20 ..... 40 30/17500 - loss: 0.8347 - accuracy: 0.3333 - val_loss: 0.8294 - val_accuracy: 0.7131
Epoch 6/20 ..... 40 30/17500 - loss: 0.8398 - accuracy: 0.4447 - val_loss: 0.8284 - val_accuracy: 0.7131
Epoch 7/20 ..... 40 30/17500 - loss: 0.8732 - accuracy: 0.5000 - val_loss: 0.8484 - val_accuracy: 0.7131
Epoch 8/20 ..... 40 30/17500 - loss: 0.7622 - accuracy: 0.5000 - val_loss: 0.8484 - val_accuracy: 0.8221
Epoch 9/20 ..... 40 30/17500 - loss: 0.8487 - accuracy: 0.5000 - val_loss: 0.8484 - val_accuracy: 0.8221
Epoch 10/20 ..... 40 30/17500 - loss: 0.8487 - accuracy: 0.5000 - val_loss: 0.8484 - val_accuracy: 0.8221
Epoch 11/20 ..... 40 30/17500 - loss: 0.8734 - accuracy: 0.4447 - val_loss: 0.8484 - val_accuracy: 0.8221
Epoch 12/20 ..... 40 30/17500 - loss: 0.8386 - accuracy: 0.5000 - val_loss: 0.8484 - val_accuracy: 0.7131
Epoch 13/20 ..... 40 30/17500 - loss: 0.8296 - accuracy: 0.5000 - val_loss: 0.8484 - val_accuracy: 0.8221
Epoch 14/20 ..... 40 30/17500 - loss: 0.8482 - accuracy: 0.7778 - val_loss: 0.8484 - val_accuracy: 0.8221
Epoch 15/20 ..... 40 30/17500 - loss: 0.8398 - accuracy: 0.5000 - val_loss: 0.8484 - val_accuracy: 0.8221
Epoch 16/20 ..... 40 30/17500 - loss: 0.8487 - accuracy: 0.5000 - val_loss: 0.8484 - val_accuracy: 0.8221
Epoch 17/20 ..... 40 30/17500 - loss: 0.8734 - accuracy: 0.5000 - val_loss: 0.8484 - val_accuracy: 0.8221
Epoch 18/20 ..... 40 30/17500 - loss: 0.8398 - accuracy: 0.5000 - val_loss: 0.8484 - val_accuracy: 0.8221
Epoch 19/20 ..... 40 30/17500 - loss: 0.8398 - accuracy: 0.5000 - val_loss: 0.8484 - val_accuracy: 0.8221
Epoch 20/20 ..... 40 30/17500 - loss: 0.8398 - accuracy: 0.5000 - val_loss: 0.8484 - val_accuracy: 0.8221
fit_metrics['loss', 'accuracy', 'val_loss', 'val_accuracy']:
Epoch 3/20 ..... 40 30/17500 - loss: 10.7153 - accuracy: 0.1000 - val_loss: 0.9171 - val_accuracy: 0.2988
Epoch 4/20 ..... 40 30/17500 - loss: 10.7111 - accuracy: 0.1000 - val_loss: 0.9171 - val_accuracy: 0.2988
Epoch 5/20 ..... 40 30/17500 - loss: 10.8259 - accuracy: 0.1000 - val_loss: 0.9171 - val_accuracy: 0.2988
Epoch 6/20 ..... 40 30/17500 - loss: 11.9972 - accuracy: 0.2000 - val_loss: 0.9171 - val_accuracy: 0.2988
Epoch 7/20 ..... 40 30/17500 - loss: 11.9972 - accuracy: 0.2000 - val_loss: 0.9171 - val_accuracy: 0.2988
Epoch 8/20 ..... 40 30/17500 - loss: 11.9972 - accuracy: 0.2000 - val_loss: 0.9171 - val_accuracy: 0.2988
Epoch 9/20 ..... 40 30/17500 - loss: 11.9972 - accuracy: 0.2000 - val_loss: 0.9171 - val_accuracy: 0.2988
Epoch 10/20 ..... 40 30/17500 - loss: 10.2023 - accuracy: 0.3000 - val_loss: 0.9171 - val_accuracy: 0.2988
Epoch 11/20 ..... 40 30/17500 - loss: 10.2023 - accuracy: 0.3000 - val_loss: 0.9171 - val_accuracy: 0.2988
Epoch 12/20 ..... 40 30/17500 - loss: 10.2023 - accuracy: 0.3000 - val_loss: 0.9171 - val_accuracy: 0.2988
Epoch 13/20 ..... 40 30/17500 - loss: 10.2023 - accuracy: 0.3000 - val_loss: 0.9171 - val_accuracy: 0.2988
Epoch 14/20 ..... 40 30/17500 - loss: 10.2023 - accuracy: 0.3000 - val_loss: 0.9171 - val_accuracy: 0.2988
Epoch 15/20 ..... 40 30/17500 - loss: 10.2023 - accuracy: 0.3000 - val_loss: 0.9171 - val_accuracy: 0.2988
Epoch 16/20 ..... 40 30/17500 - loss: 10.2023 - accuracy: 0.3000 - val_loss: 0.9171 - val_accuracy: 0.2988
Epoch 17/20 ..... 40 30/17500 - loss: 10.2023 - accuracy: 0.3000 - val_loss: 0.9171 - val_accuracy: 0.2988
Epoch 18/20 ..... 40 30/17500 - loss: 10.2023 - accuracy: 0.3000 - val_loss: 0.9171 - val_accuracy: 0.2988
Epoch 19/20 ..... 40 30/17500 - loss: 10.2023 - accuracy: 0.3000 - val_loss: 0.9171 - val_accuracy: 0.2988
Epoch 20/20 ..... 40 30/17500 - loss: 10.2023 - accuracy: 0.3000 - val_loss: 0.9171 - val_accuracy: 0.2988
    
```

Figure 10: The accuracy of the proposed framework at each iteration during the 20 epochs with activation function shown on left side and without using activation function shown in right side

Table 1: The accuracy and model loss of proposed framework with and without using activation functions

Epoch	Activation	Max Train Accuracy	Max Validation Accuracy	Max Train Loss	Max Valid Loss
15	Yes	88.89	86.58	0.8539	1.1731
20	Yes	98.88	96.72	9.5221	1.2063
25	Yes	99.7	99.3	9.9213	3.2711
15	No	71.43	24.69	13.7111	11.6169
20	No	68.33	39.60	13.7111	9.3171
25	No	77.78	60.40	6.7774	6.0383

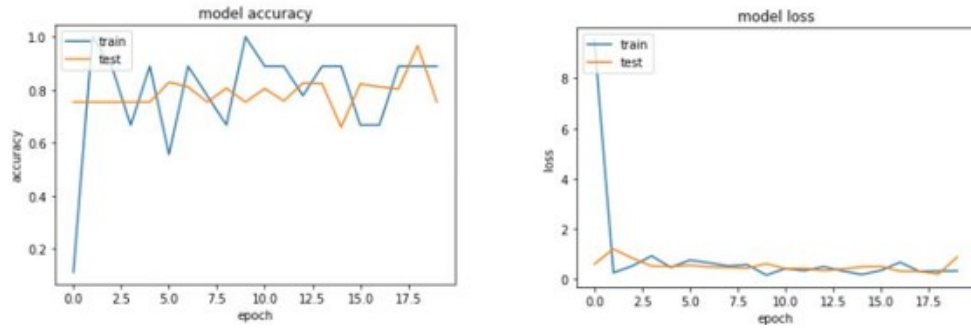


Figure 11: The graph plotting for model accuracy and loss in the proposed framework, involving the use of activation functions, was conducted over 20 epochs

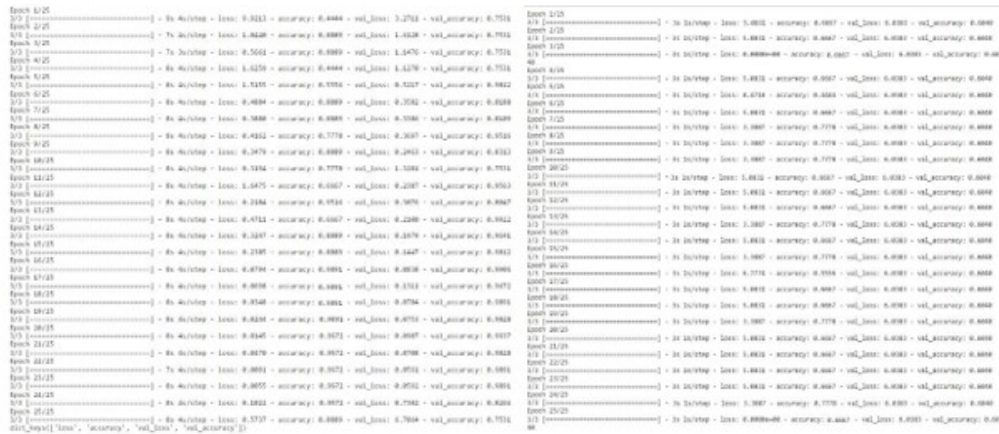


Figure 12: The accuracy of the proposed framework at each iteration during the 25 epochs with activation function shown on left side and without using activation function shown in right side

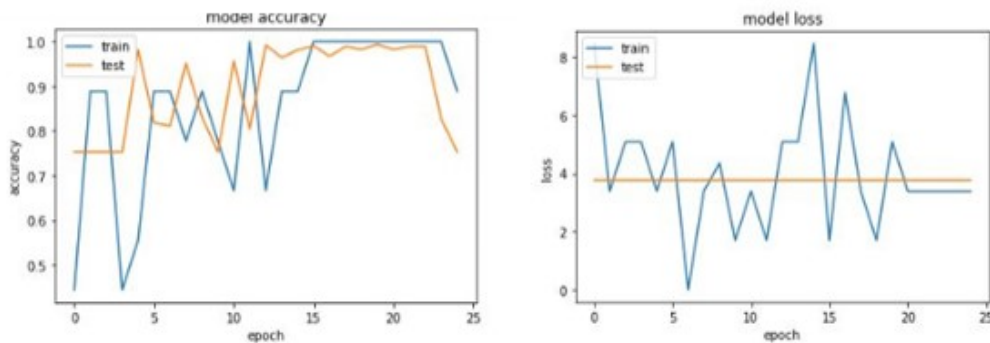


Figure 13: The graph plotting for model accuracy and loss in the proposed framework, involving the use of activation functions, was conducted over 25 epochs

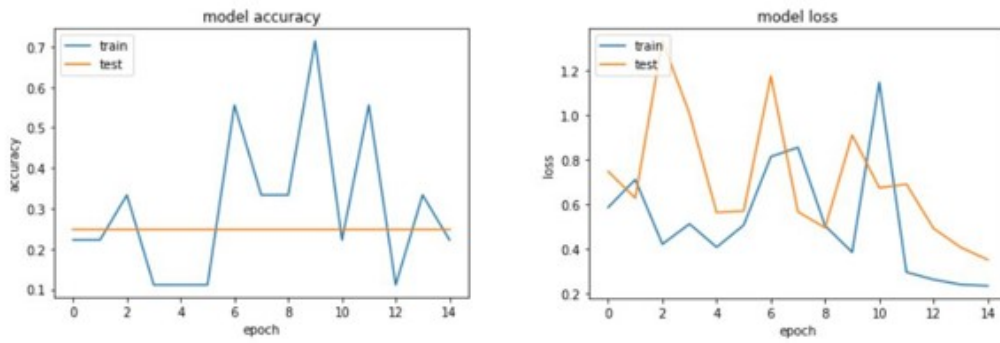


Figure 14: The graph plotting for model accuracy and loss in the proposed framework, without the use of activation functions, was conducted over 15 epochs

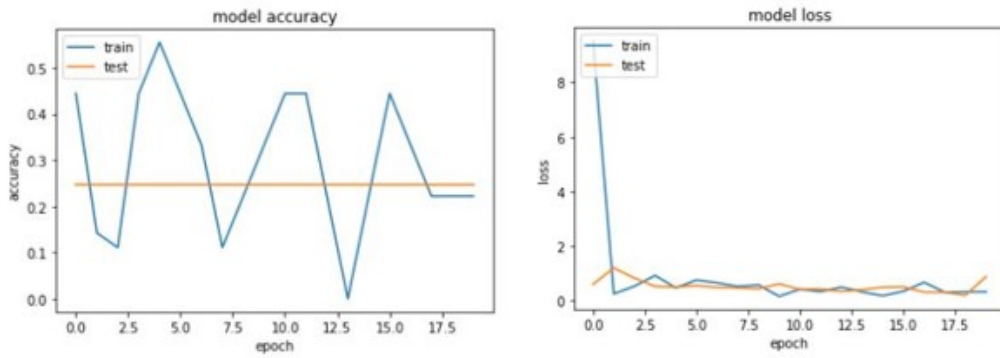


Figure 15: The graph plotting for model accuracy and loss in the proposed framework, without the use of activation functions, was conducted over 20 epochs

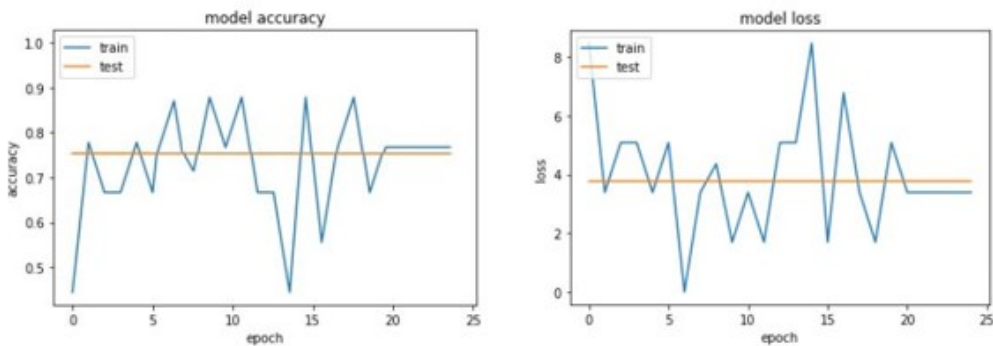


Figure 16: The graph plotting for model accuracy and loss in the proposed framework, without the use of activation functions, was conducted over 25 epochs

Table 2: Comparison of performance of the proposed framework with previous used deep learning-based model

Model	Maximum Accuracy
CNN [7]	98.5
LSTM CNN [11]	80.38
LSTM RNN [11]	82.29
VGG16 [12]	94.00
ResNet50 [12]	91.70
Proposed Framework	99.7

VGG16 and ResNet50 deep learning model networks to classifying images of breast cancer. Compared the performance of the proposed model with performance of their model, shown in table 2, and found that the proposed framework based on DNN performed better than their deep learning-based model.

6 Conclusion

In this paper, proposed a deep neural network-based framework for determining the melting point of crystalline chemical substances. Its performance evaluated in terms of training and validation accuracy, model loss, and validation loss. When comparing it to the previous model, which was based on deep learning, our framework yields the best results, with an accuracy of up to 99.7%. This suggests that a deep neural network with activation functions on higher epochs provides accurate results.

For future work, a deep learning-based model could be developed to classify images of the DCSS dataset into various chemical states, such as initial melting and partial melting, instead of just two states (complete solid or complete liquid). This would enable the extraction of more useful information from the entire melting process of crystalline chemical substances, including the initial and final melting temperature.

References

- [1] Mohd Azlan Abu, Nurul Hazirah Indra, AHA Rahman, Nor Amalia Sapiee, and Izanoordina Ahmad. A study on image classification based on deep learning and tensorflow. *International Journal of Engineering Research and Technology*, 12(4):563–569, 2019.
- [2] Zafer Acar, Phu Nguyen, and Kah Chun Lau. Machine-learning model prediction of ionic liquids melting points. *Applied Sciences*, 12(5):2408, 2022, <https://doi.org/10.3390/app12052408>.
- [3] Louis F. Fieser and Kenneth L. Williamson. Organic experiments. *Mass.: D.C. Heath*, 12(4):563–569, 1992, <http://lib.ugent.be/catalog/rug01:000277186>.
- [4] Wenlin Han and Varshil Mehta. Fake news detection in social networks using machine learning and deep learning: Performance evaluation. In *2019 IEEE international conference on industrial internet (ICII)*, pages 375–380. IEEE, 2019, <https://doi.org/10.1109/ICII.2019.00070>.
- [5] Nur Syahmi Ismail and Cheab Sovuthy. Breast cancer detection based on deep learning technique. In *2019 International UNIMAS STEM 12th engineering conference (EnCon)*, pages 89–92. IEEE, 2019, <https://doi.org/10.1109/EnCon.2019.8861256>.
- [6] Michael Masterov, Bredy Pierre-Louis, and Raymond Chuang. A computer-aided optical melting point device. *Journal of Chemical Education*, 67(3):A75, 1990, <https://doi.org/10.1021/ed067pA75>.

- [7] Florian Nigsch, Andreas Bender, Bernd van Buuren, Jos Tissen, Eduard Nigsch, and John BO Mitchell. Melting point prediction employing k-nearest neighbor algorithms and genetic parameter optimization. *Journal of chemical information and modeling*, 46(6):2412–2422, 2006, <https://doi.org/10.1021/ci060149f>.
- [8] Anurag Shrivastava and Rama Sushil. Determination of melting point of chemical substances using image differencing method. *International Journal of Software Innovation (IJSI)*, 10(1):1–10, 2022, <https://doi.org/10.4018/IJSI.297985>.
- [9] Anurag Shrivastava and Rama Sushil. An improved melting point detector algorithm for the determination of the melting point of crystalline chemical substances. In *2023 International Conference on Computer, Electronics & Electrical Engineering & their Applications (IC2E3)*, pages 1–7. IEEE, 2023, <https://doi.org/10.1109/IC2E357697.2023.10262461>.
- [10] Ganesh Sivaraman, Nicholas E Jackson, Benjamin Sanchez-Lengeling, Álvaro Vázquez-Mayagoitia, Alán Aspuru-Guzik, Venkatram Vishwanath, and Juan J de Pablo. A diversified machine learning strategy for predicting and understanding molecular melting points. *ChemRxiv2019*, pages 1–42, 2019, <https://doi.org/10.26434/chemrxiv.9914378>.
- [11] Farhana Sultana, Abu Sufian, and Paramartha Dutta. Advancements in image classification using convolutional neural network. In *2018 Fourth International Conference on Research in Computational Intelligence and Communication Networks (ICRCICN)*, pages 122–129. IEEE, 2018, <https://doi.org/10.1109/ICRCICN.2018.8718718>.
- [12] Sadasivan V. and Bami h. L. Methods for determination of melting point and melting range. *Indian standards institution (ISI)*, IS-5762-1970, 1998, <https://archive.org/details/gov.in.is.5762.1970>.
- [13] Jing Zhang, Ding Liu, and Qin-Wei Tang. The cnn deep learning-based melting process prediction of czochralski monocrystalline silicon. *IEEE Access*, 10:41986–41992, 2022, <https://doi.org/10.1109/ACCESS.2022.3168021>.